Journal of Solid State Chemistry **158,** 94–99 (2001)
doi:10.1006/jssc.2000.9102, available online at http://www.idealibrary.com on IDEAL®

The New Mercury Vanadium Phosphate $Hg_4VO(PO_4)_2$ Containing Hg_2^{2+} Dumbbells: Crystal Structure and Thermal and Magnetic Properties

E. Le Fur and J. Y. Pivan

Laboratoire de Physicochimie, Ecole Nationale Supérieure de Chimie de Rennes, Campus de Beaulieu, Avenue du Général Leclerc, 35700 Rennes, France
E-mail: jean-yves.pivan@ensc-rennes.fr

Received September 26, 2000; in revised form January 2, 2001; accepted January 19, 2001

Crystals of the title compound were obtained from hydrothermal treatments. $Hg_4VO(PO_4)_2$ crystallizes in orthorhombic symmetry with parameters $a=7.1384(2)$ Å, $b=16.6754(3)$ Å, $c=9.0797(5)$ Å, $Z=4$, and space group *Pnma* (No. 62). The crystal structure was determined from single crystal diffractometer data to residuals $R[F^2>2\sigma F^2]=0.044$, $wR(F^2)=0.050$. The VPO framework for $Hg_4VO(PO_4)_2$ is one-dimensional and consists of hexagonal tungsten bronze (HTB)-like chains of distorted vanadium octahedra that share vertices with PO_4^{3-} to generate infinite $[VO(PO_4)_2]_\infty^{4-}$ blocks as found in the structure $K_6[VO(PO_4)]_2(V_2O_3)_2(H_xP_2O_7)$. Mercury, present as Hg_2^{2+} linear dimers with $d(Hg–Hg)=2.5125(4)$ Å, ensures the connectivity between the $[VO(PO_4)_2]_\infty^{4-}$ blocks. Susceptibility measurements are consistent with V^{4+} ions and thermal behavior is explained in terms of successive disproportionation of the title compound to elemental mercury and unknown HgVPO's phases upon heating. A comparison with related *M*VPOs is presented.

Key Words: **hydrothermal synthesis; crystal structure; mercury vanadium phosphates.**

INTRODUCTION

Mercury is known to adopt various oxidation states in inorganic compounds that range from Hg^0 to Hg^{2+}, passing through monovalent Hg_2^{2+} dumbbells and polyatomic Hg_n^{x+} clusters (1). The various dimensionalities and topologies of the latter species (isolated Hg_3^{4+}, linear or planar clusters, etc.) make mercury an interesting candidate for the working out of new porous frameworks. Very little research has been devoted to Hg-containing compounds, likely because of the hazardous and poisonous properties of mercury. To the best of our knowledge, only one HgVPO phase has been reported that was obtained from high-temperature solid state reactions (2). Hydrothermal investigations of the Hg–V–P–O system have not been reported up to now. We have undertaken a systematic study of this system that resulted in the obtainment of a new porous $Hg_4VO(PO_4)_2$ with Hg_2^{2+} dumbbells. In this article, the crystal structure, thermal behavior and susceptibility data of this mercury vanadium phosphate are reported. A comparative discussion with related *M*VPOs is also presented.

EXPERIMENTAL SECTION

Synthesis and Physical Characterization

The title compound was prepared by adding 321.6 mg (1.08 mmol) of $HgSO_4$, 153.5 mg (0.84 mmol) of V_2O_5, and 57.3 mg (1.12 mmol) of V to a solution containing 1 ml. (14.4 mmol) of 85% H_3PO_4, 200 µl (3 mmol) of ethylendiamine, and 3.5 ml of distilled water. The initial mixture was placed in a Teflon-lined stainless steel autoclave (23-ml Parr instrument bomb), heated at 463 K for 60 h under autogenous pressure, and then slowly cooled to room temperature over 2 days. The final product was filtered off and recovered as a green powder containing small rod-like single crystals suitable for structural analysis. In some experiments small amounts of elemental mercury occurred. The X-ray powder pattern of the bulk was indexed using the autoindexing program Dicvol91 (3) on the basis of an orthorhombic unit cell with lattice parameters very close to those obtained from single crystal studies. Very small amounts of an unknown phase not detectable from careful examination under the microscope were also present whatever the experiment despite numerous attempts. The most intense diffraction line of this by-product occurred at $2\theta = 15.08°$ with $I/I_0 < 10\%$.

Thermogravimetric analyses were carried out on a powder sample in aluminum crucibles (12.40 mg) up to 873 K with a heating rate of 1 K/min under flowing N_2 (50 ml/min) using a Shimadzu TGA-50 thermogravimetric analyzer. Upon heating under these conditions, the title compound likely disproportionates into elemental mercury and intermediate unknown HgVPO phases (likely $Hg_3VO(PO_4)_2$ and $Hg_2VO(PO_4)_2$) that were not characterized. Magnetic susceptibility measurements were performed on a powder sample (182.3 mg) from 2 to 300 K in an applied field of 1 kg using a SHE SQUID magnetometer. The data were found

0022-4596/01 $35.00

to obey a Curie–Weiss law and were modeled using the equation $\chi = C/(T - \theta)$.

Single-Crystal X-Ray Diffraction and Structure Determination

Crystals suitable for structure determination were selected by visual examination under a microscope and then glued on thin glass fibers. Single crystal data collection has been performed at room temperature with a Nonius KappaCCD diffractometer (Centre de Diffractométrie, Université de Rennes, France) with Mo $K\alpha$ radiation ($\lambda = 0.71073$ Å). The Collect Program (4) was used to optimize the goniometer and detector angular settings during the intensity data collection that was performed in the ω–ϕ scanning mode. The entire data set was indexed, corrected for Lorentz and polarization effects, and then integrated using the Denzo program of the Kappa CCD software package (5). Frame scaling and merging of equivalents were performed using Scalepack program (5). The unit cell and the orientation matrix were refined using the entire data set of 18,884 reflections collected within the range $1 < \theta < 35°$. The crystal structure was solved using Sir97 (6) and refined against F^2 using Jana98 (7). The entire structure model was easily obtained from subsequent difference Fourier maps. Considering the crystals were roughly cylinders, numerical absorption correction was applied for the entire data set using Jana98. In the final refinement cycles, corrections for extinction effects were applied and the anisotropic displacement parameters for all atoms were refined. Further details of the data collection are listed in Table 1. Final atomic and thermal coordinates and selected bond distances and angles are listed in Tables 2 and 3. The structure drawings were produced using Diamond 2.0 (8).

TABLE 1
Crystal Data for $Hg_4VO(PO_4)_2$

I. Crystal data	
Empirical formula	$Hg_4VO(PO_4)_2$
Color; habit	Yellowish; rod-like
Crystal system	Orthorhombic
Space group	*Pnma* (No. 62)
Unit cell dimensions	$a = 7.1384(2)$ Å
	$b = 16.6754(3)$ Å
	$c = 9.0797(5)$ Å
Volume	$V = 1080.81(7)$ Å^3
Z	4
Formula weight	1059.2 g mol^{-1}
Density (calc.)	6.507 g cm^{-3}
II. Data collection, structure solution, and refinement	
Crystal size (mm^3)	$0.25 \times 0.04 \times 0.04$
Absorption coefficient	577.75 cm^{-1}
Absorption correction	Cylindrical
Maximum 2θ	$2\theta \leq 70°$
Data collected	h: 0, + 11
	k: 0, + 26
	l: 0, + 14
Unique data after merging	2454
Observed data ($F^2 > 2.0\sigma(F^2)$)	1391
Free parameters	77
$R_{int.}$	0.044
Residuals $R(F^2 > 2.0\sigma(F^2))$	0.044
wR	0.050
Extinction coefficient	0.025(1)
Min., max. (e/Å^3)	− 1.77, + 2.95
GooF	1.35

RESULTS AND DISCUSSION

The structure of $Hg_4VO(PO_4)_2$, shown in Fig. 1, is composed of vanadium octahedra and phosphorus tetrahedra interconnected to form a one-dimensional $[VO(PO_4)_2]^{4-}_{\infty}$ framework. The assymetric unit is given in Fig. 2. The examination of the interatomic bond distances and angles (Table 3) shows that the PO_4^{3-} tetrahedra are quite regular with $\bar{d}(P–O) = 1.519$ Å and the intratetrahedral angles in the range $106.6(2)° \leq 109.4° \leq 110.7(2)°$. The near neighbors of vanadium consists of the well-known distorted octahedron with the V^{4+} ion off-center toward one apex that results in a short V=O bond (dV=O = 1.657(5) Å) characteristic of the vanadyl group, a longer *trans* V- - -O bond of 2.244(5) Å and four equatorial V–O bonds of about 2 Å. The oxygen atom involved in the short and long V–O bonds (namely O3, see Table 3) is shared leading to infinite undulating chains of octahedra that propagate along the [100] direction. The bond angle V–O–V at the shared atom is 133.5°. The distances d(Hg–Hg) within the Hg_2^{2+} pairs of 2.5125(4) Å compare very well with similar distances reported for monovalent mercury oxo compounds with Hg_2^{2+} dumbbells ($\bar{d}$(Hg–Hg) = 2.514 Å) (1). The mercury atoms are bound to six (Hg1) or three (Hg2) oxygen atoms with a short Hg–O bond of about 2.1 Å (Table 3). The O2–Hg1–Hg2–O5 fragment is virtually linear with

TABLE 2
Atomic Coordinates and Equivalent Isotropic Displacement Coefficients U_{eq} (Å$^2 \times 100$) with Their Standard Deviation in parentheses for $Hg_4VO(PO_4)_2$

Atoms		x	y	z	U_{eq}
Hg1	8*d*	0.86917(3)	0.08893(1)	0.52934(3)	2.037(8)
Hg2	8*d*	0.13286(3)	0.92069(1)	0.74681(3)	2.027(8)
V	4*c*	0.6414(2)	0.25	0.7303(2)	1.08(4)
P	8*d*	0.8590(2)	0.11259(8)	0.8906(2)	1.09(4)
O1	8*d*	0.6830(5)	0.1660(2)	0.8819(5)	1.2(1)
O2	8*d*	0.8697(6)	0.0555(2)	0.7559(5)	1.9(1)
O3	4*c*	0.8575(7)	0.25	0.6636(6)	1.3(2)
O4	8*d*	0.5358(5)	0.1644(2)	0.5993(5)	1.7(1)
O5	8*d*	0.8396(5)	0.0586(2)	0.0287(4)	1.3(1)

TABLE 3
Selected Bond Lengths (Å), Bond Angles (°) with Their Standard Deviation in parentheses, and Bond Valence Sum Values (Σs) for $Hg_4VO(PO_4)_2$

	Distance	Angles					
V	O3	1.657(5)					
	O1	1.986(4)	96.5(3)				
	O1	1.986(4)	80.6(3)	89.7(2)			
	O4	2.005(4)	97.6(3)	165.8(2)	88.0(3)		
	O4	2.005(4)	97.6(3)	88.0(2)	165.8(2)	90.8(2)	
	O3	2.244(5)	176.0(3)	96.6(2)	80.6(2)	85.1(2)	97.6(2)
Σ(V) = 3.96							
P	O1	1.542(4)					
	O2	1.552(6)	110.7(2)				
	O4	1.532(6)	110.4(2)	110.6(2)			
	O5	1.550(8)	107.7(2)	106.6(2)	110.6(2)		
Σ(P) = 4.87							
Hg1	Hg2	2.5125(4)			Hg2	Hg1	2.5125(4)
	O2	2.131(4)	O5	2.876(4)		O5	2.077(4)
	O1	2.705(4)	O3	2.951(5)		O2	2.813(4)
	O4	2.766(4)				O2	2.931(4)
Σ(Hg1) = 1.06						Σ(Hg2) = 0.93	

O–Hg–Hg angles ranging from 161.1° to 172.7°. These O–(Hg_2^{2+})–O fragments run roughly along the [001] direction. The negatively charged VPO framework can be described according to $[VO^{VV}_{2/2}O^{VP}_{4/2}(PO^{PV}_{2/2}O_2)_2]$, where $O^{VV}_{2/2}$ means that each V octahedron shares two vertices with adjacent V octahedra, $O^{VP}_{4/2}$ means that each V octahedron shares four vertices with adjacent P tetrahedra, and $O^{PV}_{2/2}$ indicates that each P tetrahedron is connected through two vertices to two V octahedra. This results in infinite chains with formula $[VO(PO_4)_2]^{4-}_{\infty}$ that propagate along the [100] direction. These chains are held together via the Hg_2^{2+} dumbbells through the strong Hg–O bonds of ca. 2 Å to form layers of $Hg_4VO(PO_4)_2$ that develop in the (101) plane. The longest Hg–O bonds (dHg–O > 2.7 Å) ensure additional very weak connectivity between the layers through Van der Waals interactions. The resulting topology of the structure consists of tunnels with approximate dimensions 5×6 Å^2 that run along the *a* axis and are delimited by 2 VO_6, 4 PO_4, and 2 Hg_2^{2+} pairs (see Fig. 1). Bond valence sum calculations are in agreement with the formal oxidation states for the vanadium (Σs = 3.96), phosphorus (Σs = 4.87), and mercury centers (Σs = 1.06 for Hg1 and Σs = 0.93 for Hg1).

Thermogravimetric analysis of $Hg_4VO(PO_4)_2$ showed a total weight loss of about 37.2% that occurred in two well-separated steps with equal intensity (Fig. 3). The intermediate and final products were not identified. Making the assumption that $Hg_4VO(PO_4)_2$ disproportionates upon heating to elemental mercury and the corresponding HgVPOs, the first step was attributed to the decomposition mechanism $Hg_4VO(PO_4)_2 \xrightarrow{\Delta} Hg_3VO(PO_4)_2 + Hg^0$ while the second one corresponds to $Hg_3VO(PO_4)_2 \xrightarrow{\Delta} Hg_2VO(PO_4)_2 + Hg^0$. Though the formula of the decomposition products $Hg_3VO(PO_4)_2$ and $Hg_2VO(PO_4)_2$ remains speculative, the mechanisms that are proposed appear to be reasonable. Further temperature-dependent X-ray diffraction (TDXD) studies are planned to elucidate the decomposition mechanisms and to identify the resulting products. Magnetic susceptibility data were found to obey a Curie–Weiss law and were equated according to $\chi = C/(T - \theta)$. A fit to the experimental magnetic data, represented in Fig. 4, gave values of $C = 0.591$ emu-K/mol. ($\theta = 0.6$ K). The difficulty in obtaining a sample free of small amounts of impurity (see Experimental Section: *Synthesis and Physical Characterization*) made an accurate interpretation of the magnetic data rather illusive. However, the calculated magnetic moment per vanadium atom is consistent with the bond valence sum calculations obtained from the structural study.

The structure of $Hg_4VO(PO_4)_2$ contains infinite chains of octahedra that are present in other MVPO compounds such as $M_6[VO(PO_4)_2]_2(V_2O_3)_2(H_x(P, V)_2O_7)$ ($M = K^+$, Tl^+, Rb^+, NH_4^+) and related phases (9–12), $K_2(VO)_3(HPO_4)_4$ (13) and $M_{\sim 5}(VO)_{10}(PO_4)_4(HPO_4)_8$ ($M = Cs^+$, Rb^+, Tl^+, NH_4^+) (14). Different kinds of VOV bond angles occur at the shared oxygen atoms in connection with geometric restraints associated with the nature and/or the number of VO_6/PO_4 links along the chains (Fig. 5). When phosphate groups link two adjacent octahedra along the chain, $[VO_5]_\infty$ HTB-type chains are formed with VOV

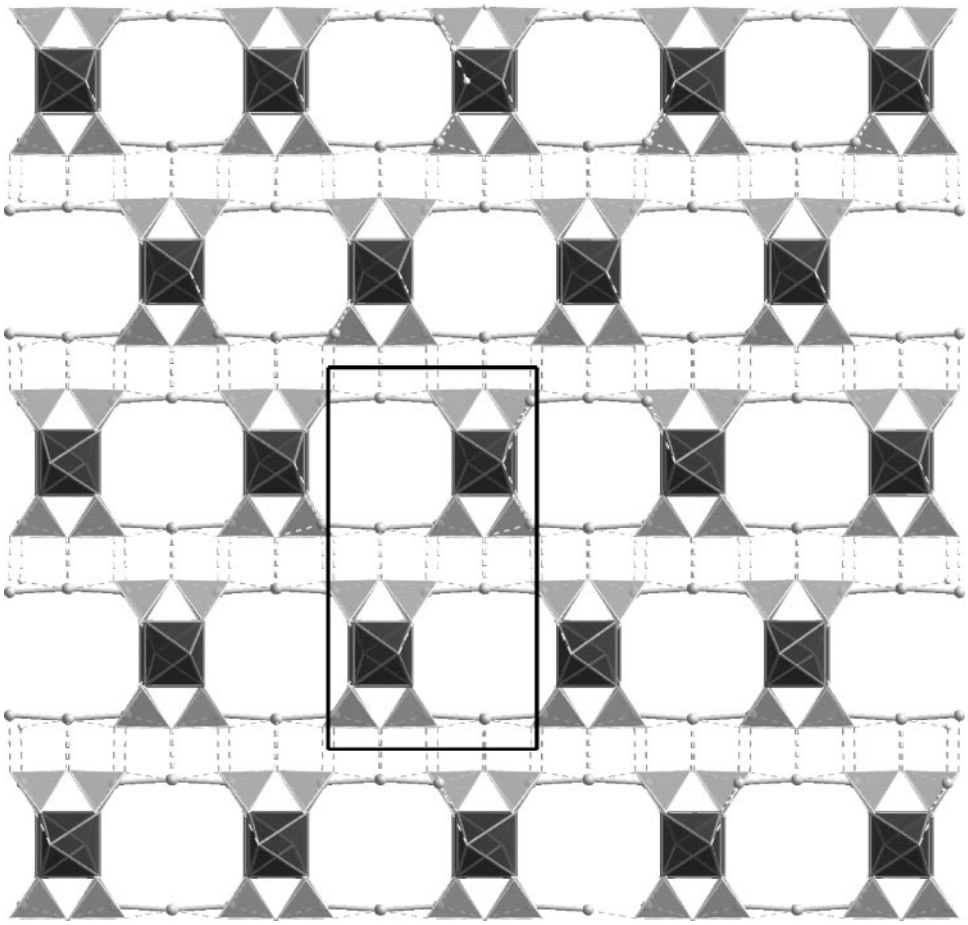

FIG. 1. View of $Hg_4VO(PO_4)_2$ along the [100] direction. The black polyhedra are the VO_6 octahedra; the grey ones are the PO_4 tetrahedra. The mercury atoms are represented as grey spheres. The Hg–Hg bonds within the Hg_2^{2+} pairs are solid grey lines. The weak contacts between the layers of $Hg_4VO(PO_4)_2$ are shown as dotted lines. The unit cell is emphasized.

angles at the shared O atoms ranging from $\sim 146^\circ$ (one PO_4 bridge) to $\sim 132^\circ$ (two PO_4 bridges). On the contrary, the VOV angle is much higher with values in the range $\sim 156^\circ$–173° with *quasi*-linear ReO_3-type chains when

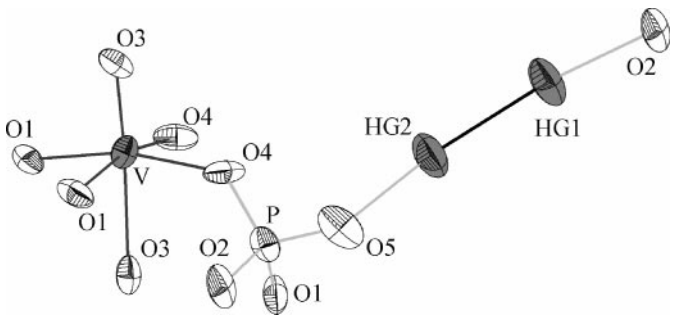

FIG. 2. View of the asymetric unit of $Hg_4VO(PO_4)_2$ (Ortep-style) showing the connectivity. Thermal ellipsoïds are at the 95% probability level.

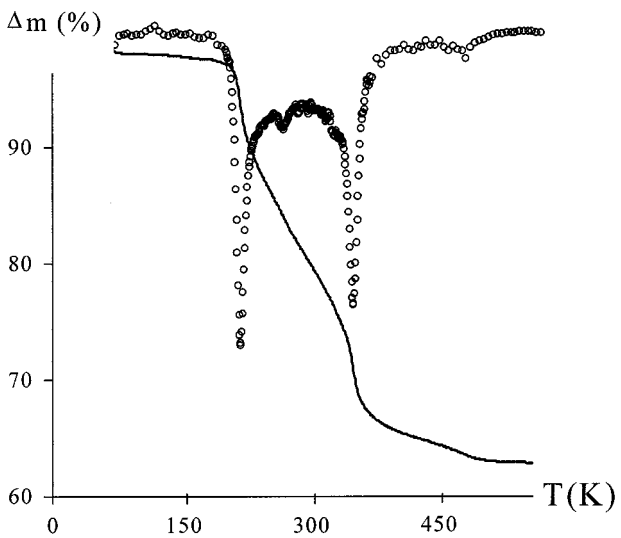

FIG. 3. Thermogravimetric curve for $Hg_4VO(PO_4)_2$.

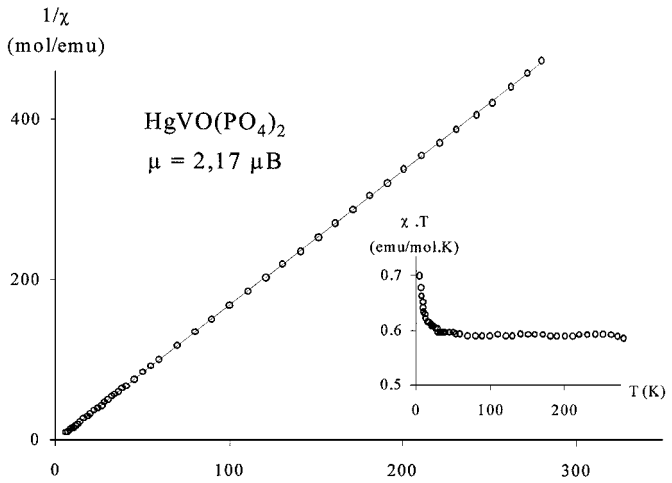

FIG. 4. χT and $\chi^{-1} = f(T)$ curves for $Hg_4VO(PO_4)_2$.

there are not phosphate bridges between adjacent octahedra. Both types of chains are present in the structures $K_2(VO)_3(HPO_4)_4$ and $M_{\sim 5}(VO)_{10}(PO_4)_4(HPO_4)_8$ but only the HTB-like chains occur in the structures $Hg_4VO(PO_4)_2$ and $M_6[VO(PO_4)_2]_2(V_2O_3)_2(H_x(P, V)_2O_7)$. For the latter two structures, the HTB-like chains are linked to the tetrahedra to generate isoformular one-dimensional $[VO(PO_4)_2]_\infty^{4-}$ blocks. As is readily seen in Fig. 6, these blocks are not identical for the two structures due to different orientations of the phosphate groups with respect to the chains. The connectivity between the $[VO(PO_4)_2]_\infty^{4-}$ blocks is ensured by $(V_2O_3)_2H_x(P, V)_2O_7$ units in the case of

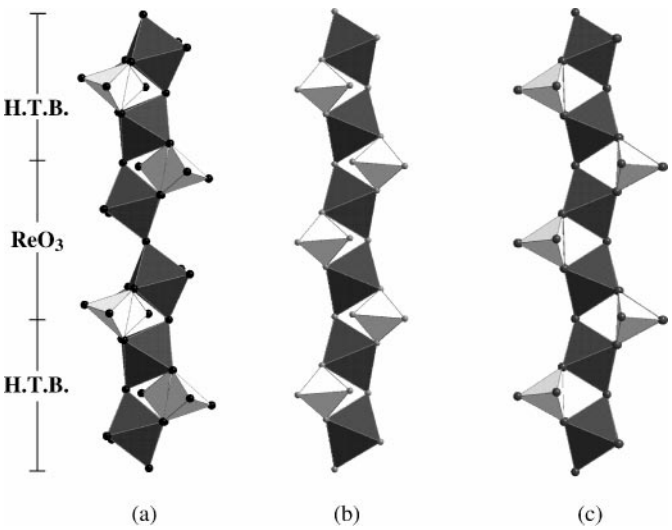

FIG. 5. The different types of VO_6/PO_4 links along the chains of octahedra. The HTB. and ReO_3 units along the chains are emphasized (a); the chain as found in $Hg_4VO(PO_4)_2$ (b); and the chain as found in $M_6[VO(PO_4)_2]_2(V_2O_3)_2(H_x(P, V)_2O_7)$ (c).

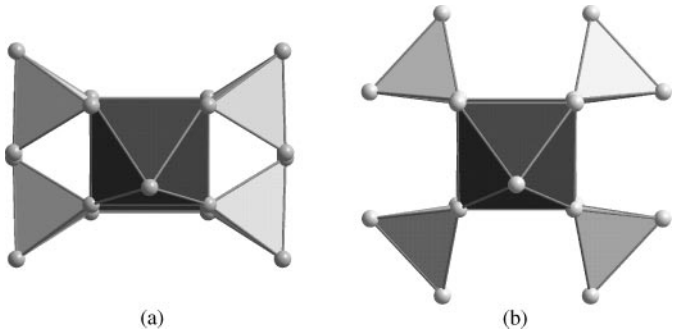

FIG. 6. The unit $[VO(PO_4)_2]$ viewed along the axis of propagation of the [VO] chain in $Hg_4VO(PO_4)_2$ (a) and in $M_6[VO(PO_4)_2]_2(V_2O_3)_2(H_x(P, V)_2O_7)$ (b).

$M_6[VO(PO_4)_2]_2(V_2O_3)_2(H_x(P, V)_2O_7)$ and results in an overall 3D framework with the M^+ cations located inside tunnels. On the contrary, the highly anisotropic Hg_2^{2+} pairs make links only along the c axis between adjacent $[VO(PO_4)_2]_\infty^{4-}$ blocks and result in the layered neutral framework $Hg_4VO(PO_4)_2$ with weak interactions between the layers.

CONCLUDING REMARKS

The new $Hg_4VO(PO_4)_2$ has been obtained from soft hydrothermal treatments. Its structure has been refined in orthorhombic symmetry (space group *Pnma*) from X-ray single crystal diffraction data and consists of $[VO_5]_\infty$ HTB-like chains connected through phosphate groups to Hg_2^{2+} pairs to form a tunneled structure. The title compound is thought to disproportionate in two steps to elemental mercury and the unknown $Hg_3VO(PO_4)_2$ and $Hg_2VO(PO_4)_2$ phases from thermogravimetric measurements. Susceptibility measurements indicate that there are no significant magnetic interactions between the vanadium centers.

ACKNOWLEDGMENTS

The authors are indebted to Dr. T. Roisnel for the single-crystal intensity data collection on the Kappa CCD diffractometer and to Dr. O. Peña for the susceptibility measurements (LCSIM, UMR 6511, Université de Rennes, France).

REFERENCES

1. N. V. Peruvkhina, S. A. Margarill, S. V. Borisov, G. V. Romanenko, and N. A. Pal'chik, *Russ. Chem. Rev.* **68**(8), 615 (1999).
2. S. Boudin, A. Grandin, A. Leclaire, M. M. Borel, and B. Raveau, *J. Mater. Chem.* **4**(12), 1889 (1994).
3. D. Louër and M. Boultif, *J. Appl. Crystallogr.* **24,** 987 (1991).
4. Collect: KappaCCD Software. Nonius BV, Delft, The Netherlands, (1998).

5. Z. Otwinowski and W. Minor, *in* "Methods in Enzymology" (C. W. Carter, Jr., and R. M. Sweet, Eds.), New York Academic Press, pp. 307–326 (1997).
6. A. Altomare, M. C. Burla, M. Camalli, G. Cascarano, C. Giacovazzo, A. Guagliardi, A. G. G. Moliterni, G. Polidori, and R. Spagna, *J. Appl. Crystallogr.* **32,** 115 (1999).
7. V. Petricek, Jana-98, crystallographic computing system for ordinary and modulated structures, 1998.
8. K. Brandenbourg, Diamond 2.0, 1998.
9. G. Huan, J. W. Johnson, A. J. Jacobson, E. W. Cormoran, and D. P. Goshorn, *J. Solid State Chem.* **93,** 515 (1991).
10. L. Benhamada, A. Grandin, M. M. Borel, A. Leclaire, and B. Raveau, *J. Solid State Chem.* **110,** 305 (1991).
11. J. T. Vaughey, W. T. A. Harrison, and A. J. Jacobson, *J. Solid State Chem.* **110,** 305 (1994).
12. E. Le Fur, B. de Villars, J. Tortelier, and J. Y. Pivan, *Int. J. Inorg. Mater.* **3**(1), 9 (2001).
13. K. H. Lii and H. H. Tsai, *J. Solid State Chem.* **91,** 331 (1991).
14. E. Le Fur, B. de Villars, J. Tortelier, and J. Y. Pivan, *Inorg. Chem.* **40**(2), 272 (2001).